CHARACTERIZING POLAR LAYERED DEPOSITS AT THE MARTIAN NORTH POLE: CURRENT RESULTS AND TECHNIQUES. S. M. Milkovich and J. W. Head, III, Dept of Geological Sciences, Brown University, Providence, RI 02912. Sarah_Milkovich@brown.edu

Introduction: Within the northern residual polar cap of Mars are dark lanes or troughs; on the walls of these exposures are layered deposits. These deposits consist of extensive lateral layers of ice and dust and are found throughout the polar cap. They were first identified in Mariner 9 images [1, 2] and later studied in detail with the Viking orbiters [e. g. 3, 4, 5, 6]. In these images, the layers appear to consist of alternating sequences of light and dark layers ~ 5 to 25 m thick [4, 5]. Recent data taken by the Mars Orbiter Camera (MOC) onboard the Mars Global Surveyor (MGS) reveal that the layers are thinner and more numerous than Viking images suggested. Layers are seen with thicknesses at the limit of resolution (~2 m) and it is possible that smaller scale layers may also exist [7].

An understanding of the formation processes of the polar layered terrain will provide insights into the processes of trough formation, lateral propagation, erosion, and deposition. It will also allow us to interpret the simple vertical record of climate change encoded in the layered deposits. Ultimately, we will gain a foundation upon which we can build a better model for the interactions of the various volatile deposits on Mars, including the current polar surface as well as the latitude-dependent layer of subsurface ice currently being mapped by Mars Odyssey [8, 9].

In order to begin this foundation of knowledge we first must characterize sections of layers and quantitatively compare the layer sequences in one trough with another. In this way, constraints may be placed on trough formation mechanisms.

Polar Trough Characterization: Much work has been done to describe the layers in the northern cap, especially those in the region shown in Figure 1.

The individual layers show considerable variation in thic k-ness and conformity. Layers range in thickness from several meters to several tens of meters [10]; some layers are observed to pinch out [7]. Additionally, layers show varying resistance to erosion. In particular, a "marker bed" 20 m thick with resistant knobs ~ 10 m wide is observed in many places [7, 11, 12]

Layers also show variation in surface texture. Individual layers display surfaces with pockmarks, brick-like textures, and a pattern similar to a deformed, woven structure [10]. It is not clear if the textures are a property of the layer or are limited to the exposed surface. There is not a relation between texture and location. The variety of textures may be due to structural properties of the individual layers which caused different amounts of erosion [10]. Some textures indicate a pitted surface, which may be due to outgassing of clathrate-rich layers [12].

These layers are laterally extensive. Several images taken from a Trough A in Figure 1 show that in some regions individual layers can be traced for many hundreds of kilometers [7, 12]. Two different investigators have proposed that the marker bed can be found in multiple troughs 50 km apart [7, 11]. However, a preliminary assessment of images found that layer sequences vary greatly around the cap [10]. An additional difficulty for comparing image sequences is the seasonal surface frost deposits found throughout this area. Indeed, two sequences can look very different from each other when in reality they are taken from either side of the same image [12]. Frost can cause several layers to look like one thick layer. It can also be preferentially deposited within a segment of a dark region, revealing many layers in an area which would otherwise be thought to be one layer [12].

Figure 1c shows image M00-01754 from Trough A. Figure 1d is the DN profile taken along the dashed line in 1c. Some layer transitions are seen as sharp jumps in the DN profile; the most distinct of these are identified with letters in the two images. The region of the image above layer *a* clearly contains several layers. However, when examining the DN profile there are no clear jumps in DN value that indicate a layer boundary. Additionally, there is more variation in brightness within the light layer above *a* than our eyes can observe from the image. The DN profile reveals details about the layers that might otherwise be missed.

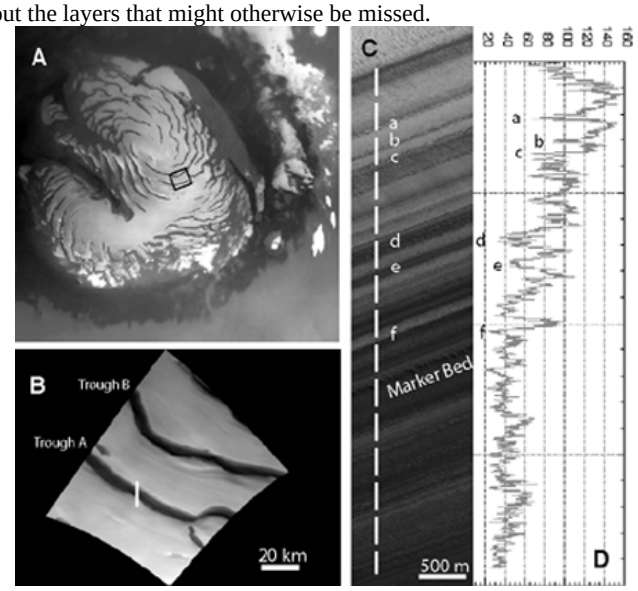

Figure 1. Layers in the Northern Cap. A) Northern polar cap. Box indicates location of 1B. B) Two troughs in the cap. Line indicates location of 1C. C) Subframe of image M00-01754. Dashed line indicates location of DN profile in 1D. Sun is from upper right. D) DN profile from image.

Many models were proposed for the formation of these deposits based on Viking data [e.g., 13, 5] but the details of the formation process remain unknown. The main driving force behind the deposits is thought to be episodic climate variations due to orbital cycles. Indeed, some effort has been made to connect layers to specific orbital cycles, especially obliquity, using computer models [4, 14] and spectral signal analysis [15]. However, the variability

of individual layers may indicate the influence of smaller scale variations. Such variations may include the influence of local topography or non-uniform deposition of material such as ejecta from major impacts or pyroclastic material [10]. Additionally, the thinner layers may indicate that the martian climate produces deposits on timescales less than the obliquity cycle [7]. Thus, characterization of cycles within layers without relying on specific orbital periods is a necessary first step before introducing process-specific factors.

Characterization Using Fourier Analysis: One-dimensional Fourier analysis is used to break a complex signal down into sine and cosine components [16]. Dominant wavelengths of the complex signal can be measured from these components. The Fourier transform is described by the following equation:

$$F(k_x) = \int_{-\infty}^{\infty} f(x) e^{-ik_x x} dx \qquad (1)$$

where $k_x = 2\pi/\lambda$ is the spatial wavenumber. Spatial frequency, $k_x/2\pi$, can be inverted to find spatial wavelength, $\lambda = 2\pi/k_x$. The power spectrum of the signal is described by:

$$P(k_x) = \int_{-\infty}^{\infty} \left| F(k_x) \right|^2 dk_x \qquad (2)$$

A fast Fourier transform (FFT) is a discrete form of equation (1) and is computed numerically. Plots of spatial frequency vs. relative power were created using the FFT function in the Matlab package software; these plots were then inverted to determine spatial wavelengths. The same method and program were used as is described in [16].

Applying FFTs to the PLD: The polar layered deposits record a complex signal of changing depositional environments in their layers. FFTs may be a valuable tool to characterize how the depositional environment varied from location to location.

To be a useful tool for comparing images, FFTs must return similar results from layer sequences which are practically identical. Previously, we have performed FFT analysis on many profiles from a single image, M00-01754. Profiles from either side of this image yielded very similar dominant wavelengths, as was expected. However, the dominant wavelength varied down the length of the trough wall exposure. This may be due to compression of the layers towards the base of the deposit from the overlying material or to a change in the depositional environment [17].

The next step of this analysis is to compare the FFTs of DN profiles from multiple images. In order to do so, the FFT program has been adapted to compensate for slope angle of the trough wall. MOLA data and MOC images are correlated using the ISIS image processing package, and the MOLA data is interpolated between shots to provide an elevation value for each pixel of the image. Thus, the exposure of layers in the image is projected back onto the vertical wall of the trough. Next this data set is adjusted so that it consists of DN values at locations spaced evenly down the vertical wall. This process interpolates between DN values for neighboring pixels; while this may not be a true assumption at the boundaries between layers, the pixel size is small (1.6 m/pxl) that the errors introduced are negligible. The interpolations were done using the Arand suite of programs developed at Brown University for paleoceanographic studies. Evenly spaced data is required for the FFT process; the adjusted data is then run through the Matlab FFT program.

The new process has been run on image M00-01754. The dominant wavelengths found in M00-01754 are approximately 20 m, 25 m, and 30 m (Figure 2). Laskar et al [15] have also analyzed cycles within an image from Trough A. They observed three similar regions whose boundaries correspond to layers *c*, *d*, and *f* in Figure 1c. These regions formed the cycles which they correlated with insolation variations dominated by precession. Laskar et al's deposition cycle may be the same as our 30 m cycle; this implies that additional cyclic forces are influencing the deposition of the layered material on shorter timescales than those discussed in [15].

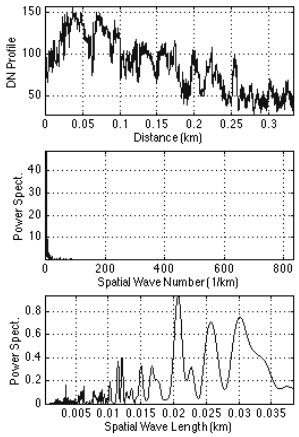

Figure 2. FFT of image M00-01754.

Two additional images are selected for this process; M00-02100 is located in the same trough as M00-01754, and M00-01714 is found in a nearby trough (Trough B in Figure 1). Results from the additional images are forthcoming.

Discussion: Characterization of the layered deposits is key to our understanding of the processes which shape the polar regions and the martian climate as a whole. We have characterized the layers within a single trough in the northern cap. Fourier analysis provides a useful tool to assist in comparisons of layer sequences. Additionally, Fourier analysis will allow us to pull out the cycles within these sequences which can then be used to constrain the processes which deposited these layers and shaped the troughs. These efforts in turn will aid our understanding of the martian climate system.

Acknowledgments: *Thanks are extended to Timothy Herbert and Phillip Howell of Brown University for providing the Arand programs.*

References: [1] Soderblom L., et al. (1973) *JGR 78,* 4197-4210. [2] Cutts J. A. (1973) *JGR 78*, 4231-4249. [3] Kieffer H. H. et al, (1976) *Science 194* , 1341-1344. [4] Blasius K. R., et al. (1982) *Icarus 50*, 140-160. [5] Howard A. D., et al. (1982) *Icarus, 50,* 161-215. [6] Thomas P. C. et. al. in *Mars* [ed.by H. H. Kieffer et al] pp.767-795. Univ. of Arizona Press, Tuscon. [7] Malin M. C., Edgett K. S. (2001) *JGR 106,* 23429-23570. [8] Mitrofanov, I. et al (2002) *Science 297,* 78-81. [9] Boynton, W. V. et al (2002) *Science 297,* 81-85. [10] Milkovich, S. M., Head J. W. (2001) LPSC 32, #1976. [11] Kolb E. J., Tanaka K. L (2001) *Icarus 154,* 22-39. [12] Milkovich, S. M., Head, J. W. (2002) LPSC 33, 1713. [13] Squyres, S. W. (1977) *Icarus 40,* 244-261. [14] Cutts, J. A., Lewis, B. H. (1982) *Icarus50,* 216-244. [15] Laskar, J., et al. (2002) *Nature 419,* 375-377. [16] Patel, J. G., et al (1999) *JGR 104*, 24057-24074. [17] Milkovich, S. M., Head J. W. (2001) Microsymposium 36, #ms069.